limit of integration in (1) is x, the effects of backscatter are excluded. That is, to include the effects of backscatter, the range of integration would have to include the entire terrain. Also, the integral equation in (1) neglects the effects of side-scatter since the derivation of (1) assumed ridges uniform in the direction transverse to the propagation direction. In the case of small slopes and the transmitting antenna near the earth, side-scatter and backscatter are second order effects.

3. EXAMPLES

In this section we examine the behavior of the attenuation function, f(x), for eight terrain profiles, y(x). Comparisons of results from (1) with previous results for a flat earth, a smooth homogeneous cylindrical earth, a smooth sea-land-sea path and a single Gaussian-shaped ridge seem to validate the technique. Its more general applicability is illustrated by calculations for propagation over two Gaussian hills, over an island that rises above sea level, and over a sea-sloping beach with a sand-dune path.

3.1 A Flat Earth

$y(x) = 0$, $y'(x) = 0$. The solution of the integral equation (1) is trivial and is simply

$$f(x) = W(x), \tag{2}$$

where $W(x)$ is the Sommerfeld flat-earth attenuation function (Wait, 1964).

3.2 A Parabodoidal Earth

$y(x) \cong -x^2/2a$, $y'(x) = -x/a$, where a is the radius of the cylinder and is taken to be about 6.37×10^3 kilometers. The frequency of the transmitting antenna is 1 MHz and is vertically polarized. The ground constants are: $\sigma = 0.01$ mho/m and $\epsilon_r = 10$. The magnitude and phase of the attenuation function versus horizontal distance, x are given in table I. These results are compared in table I with those

obtained using the residue series (Wait, 1964) for the attenuation function. The agreement is seen to be very good out to the largest distance computed. For example, at 300 km, the difference in the phase between the integral equation method and the residue series method is about 0.009 rad. or about 0.5°. The greatest error in amplitude occurs at a distance of 150 km and is about 2 units in the third significant figure. The error decreases on either side of this point, a characteristic common to many numerical solutions. The results obtained in table I are for a step size, h = 1 km; however, a step size of 2 km did not change the results appreciably. A detailed error analysis is beyond the scope of this paper. The last significant figure of agreement in table I is underlined.

Table I. Attenuation function versus distance

Horizontal Distance, x (km.)	Integral Equation Solution		Residue Series Solution	
	Amplitude	Phase (rad.)	Amplitude	Phase (rad.)
0	1.0	0	1.0	0
25	0.51331	-1.9717	0.51332	-1.9709
50	0.28936	-2.5929	0.28970	-2.5921
75	0.17575	-2.9597	0.17595	-2.9556
100	0.11506	3.0902	0.11520	3.0892
125	0.08044	2.9126	0.08000	2.9131
150	0.05914	2.7606	0.05939	2.7663
175	0.04504	2.6169	0.04502	2.6120
200	0.03512	2.4736	0.03509	2.4680
225	0.02781	2.3278	0.02777	2.3213
250	0.02224	2.1780	0.02221	2.1710
275	0.01790	2.0249	0.01788	2.0168
300	0.01447	1.8681	0.01446	1.8591

The time required to compute the attenuation function at intervals of one kilometer out to a maximum distance of 300 km was about 25 min using a CDC 3800 computer. The time required to compute the attenuation function for a specified profile is approximately proportional to the square of the number of points used along the abscissa. Thus, in the above example, if the maximum distance were 150 km rather than 300 km, the time required would be about 1/4 as much, or about 6 min. The sample input and output data given in appendix C pertain to this sample.

3.3 A Gaussian-Shaped Ridge

$y = e^{-(x-5)^2}$, $y' = -2(x-5)y$. This is a more interesting profile at least from the standpoint of radio propagation. The profile together with the magnitude of the attenuation function versus distance are shown plotted in figure 3. The magnitude of the attenuation function $|f(x)|$, is normalized to twice the free space field, $2\exp(-ikr_o)/r_o$. The observer is located on the terrain and the transmitter is located at the coordinate origin. The ground constants are $\sigma = 0.01$ mho/m and $\epsilon_r = 10$. The transmitter is vertically polarized and the frequency is 1 MHz. The terrain profile shown in the insert has a maximum height of 1 km and the hill is centered at a point 5 km from the transmitter. The solid straight line in figure 3 is the attenuation function, $W(x)$, for a flat earth.

The data in figure 3 represented by crosses was obtained by replacing the Gaussian-shaped ridge with a rounded knife-edge and computing the field on the surface shown dashed in figure 4 using "4-ray theory" (Schelleng, et. al., 1933). The radius of the rounded knife-edge is 500 m (which is the curvature of the Gaussian

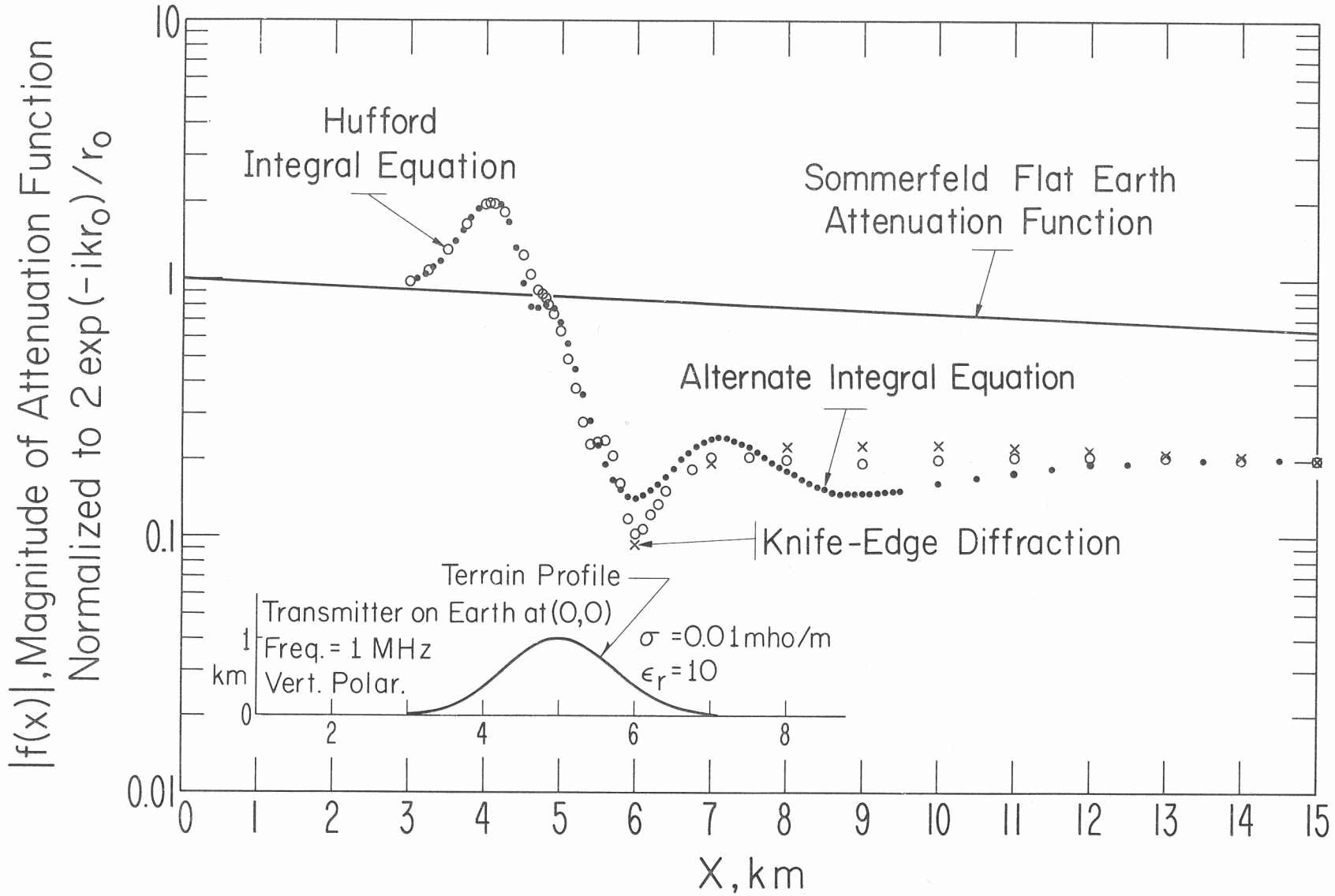

Figure 3. Propagation over a Gaussian-shaped ridge. Terrain profile is shown in insert. Observation point (receiving antenna) is located on the profile.

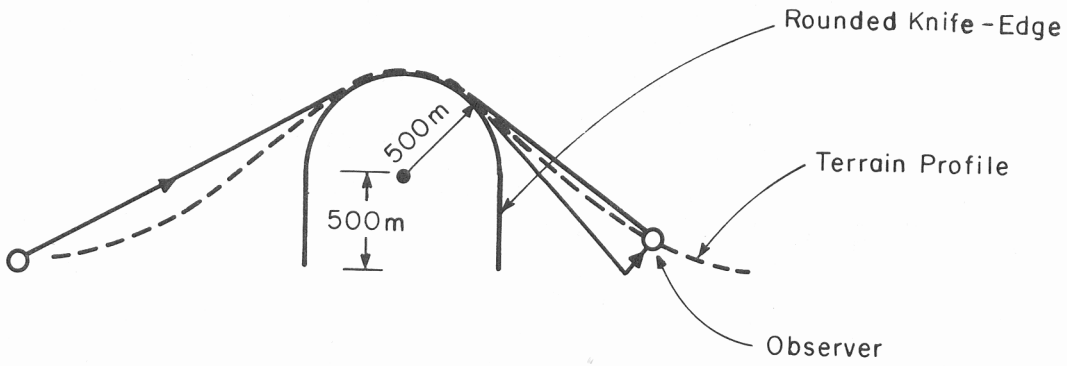

Figure 4. Rounded knife-edge approximation used to analyze the Gaussian-shaped ridge.

hill at its crest) and the knife-edge is located 1 km above the plane $y = 0$. The four rays are the two rays that strike the knife-edge on the illuminated side plus the two rays that reach an observer in the shaded side i.e., a direct diffracted ray and a ray which is diffracted and then reflected before reaching the observer. The results in figure 3 show excellent agreement between the points computed using "4-ray theory" and those obtained solving the integral equation numerically.

The open circles in figure 3 were computed using the Hufford integral equation (Hufford, 1952). Since there are fewer approximations in the Hufford integral equation than in the results presented in this paper, the former should be considered the most accurate. Hufford's integral equation shows a slight dip in the attenuation function at a distance of about 9 km which is exaggerated by the solid circles but does not appear in the knife-edge results. Also, the open circles differ somewhat in the shadow from the results presented earlier by Berry (1967). There were projection factors, of the form $\sqrt{1 + (y')^2}$, omitted from Berry's results since in most applications these factors are nearly unity, i.e., y' is small. However, in the present example these factors become important.

The solid circles in figure 3 present the attenuation function computed numerically using the integral equation in (1). We find some error in the results obtained using the integral equation presented in this paper around 6 km and 9 km. However, the error is small and is exaggerated in this particular example because of the large slopes encountered on the terrain profile. The error is a result of the assumption that

$$\frac{\partial^2 \psi}{\partial x^2} \cong 0 \ ,$$

or that the fast phase variation of φ with x is in the term $\exp(-ikx)$. In most terrain profiles, this will indeed be a good approximation and, in fact, in the present example yields adequate accuracy.

The physical characteristics of the results in figure 3 are interpreted most easily using the ray picture. The attenuation function decreases at the flat earth rate for the first $2\frac{1}{2}$ km. Then, as the observation point moves up the crest of the hill, the attenuation function increases due to focusing of the direct ray and the surface ray on the lit side of the crest. The attenuation function reaches its maximum value very close to the point on the terrain where there is an inflection point. This increase in the amplitude to a maximum on the lit side near the crest has also been predicted analytically by Wait and Murphy (1958). Just over the top of the hill the attenuation function decreases since the direct ray is no longer present and then the attenuation function partially recovers again due to the constructive interference of a direct diffracted ray and a diffracted ray traveling along the surface before reaching the observer.

3.4 A Sea-Land-Sea Path

The terrain profile is flat in this example and the ground constants change abruptly at the sea-land, land sea interfaces. This example was selected as a check on the mixed path capabilities of the method. The results for the magnitude of the attenuation function normalized to twice the free space field are plotted in figure 5 versus distance from the antenna in km. The antenna is vertically polarized and the frequency is 10 MHz. The solid circles represent the attenuation function computed numerically using (1). The open circles in figure 5 represent the attenuation function computed by Rosich (1968, 1970) using a perturbation approach. The data given by the crosses in figure 5 represents the attenuation function computed using a method based upon the classical residue series (Furutsu, et. al., 1964). This method is equivalent to that of Wait (1964). This latter method makes the fewest approximations for the three section earth considered in